

# SELF-CONSISTENT COMPUTATION OF ELECTROMAGNETIC FIELDS AND PHASE SPACE DENSITIES FOR PARTICLES ON CURVED PLANAR ORBITS \*

G. Bassi, University of Liverpool, J. A. Ellison <sup>†</sup>, K. Heinemann, University of New Mexico, M. Venturini, LBNL, and R. Warnock, SLAC

## Abstract

We discuss our progress on the self-consistent calculation of the 4D phase space density (PSD) and electromagnetic fields in a Vlasov-Maxwell formulation. We emphasize Coherent Synchrotron Radiation (CSR) from arbitrary curved planar orbits, with shielding from the vacuum chamber, but space charge forces are naturally included. Our focus on the Vlasov equation will provide simulations with lower numerical/statistical noise than standard PIC methods, and will allow the study of issues such as emittance degradation and microbunching due to space charge and CSR in bunch compressors. The fields excited by the bunch are computed in the lab frame from a new double integral formula. The field formula is derived from retarded potentials by changes of variables. It is singularity-free and requires no computation of retarded times. Ultimately, the Vlasov equation will be integrated in beam frame coordinates using our method of local characteristics. As an important intermediate step, we have developed a “self-consistent Monte Carlo algorithm”, and a corresponding parallel code. This gives an accurate representation of the source and will help in understanding the PSD support. In addition we have (1) studied carefully a 2D phase space Vlasov analogue and (2) derived an improved expression of the field of a 1D charge/current distribution which accounts for the interference of different bends and other effects usually neglected. Bunch compressors will be emphasized.

## INTRODUCTION

Our basic starting point is the Vlasov-Maxwell system in 6D, i.e., we assume collisions can be ignored and that the  $N$ -particle bunch can be approximated by a continuum. Our coordinate system,  $(Z, X, Y)$ , is shown in Fig. 1. We assume an external force due to a magnetic field,  $B_{ext}(\mathbf{R})$ , in the  $Y$ -direction. We define a reference orbit,  $\mathbf{R}_r(s) = (Z_r(s), X_r(s))$ , lying in the  $Y = 0$  plane, which is a solution of the Lorentz equation for  $\mathbf{E} = 0$  and  $\mathbf{B} = B_{ext}(\mathbf{R})\mathbf{e}_Y$ . Here  $\mathbf{R} := (Z, X)$  and  $s$  is arc length along the reference orbit. In Fig. 1 we sketched  $\mathbf{R}_r(s)$  for a 4 dipole magnetic chicane bunch compressor. We focus on the evolution of  $\mathcal{E} := (E_Z, E_X, B_Y)$  and take  $(E_Y, B_Z, B_X) = 0$ . We model shielding by the vacuum chamber by taking  $\mathcal{E} = 0$  at  $Y = \pm g$ , where  $h = 2g$  is the height of the vacuum chamber as shown

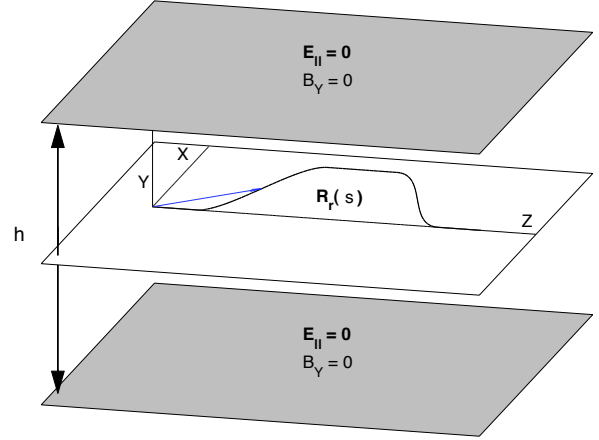


Figure 1: Basic lab frame setup.

in Fig.1. We let  $H(Y)$  be the fixed  $Y$  density defined for  $|Y| \leq g$ , then the coupled 4D Vlasov-Maxwell system for the field vector  $\mathcal{E}(\mathbf{R}, Y, u)$  and the phase space density  $H(Y)\delta(P_Y)\Psi(\mathbf{R}, \mathbf{P}, u)$ , with the shielding boundary condition, takes the form:

$$\square \mathcal{E}(\mathbf{R}, Y, u) = H(Y)S(\mathbf{R}, u), \quad (1)$$

$$\partial_u \Psi + \dot{\mathbf{R}} \cdot \nabla_{\mathbf{R}} \Psi + \dot{\mathbf{P}} \cdot \nabla_{\mathbf{P}} \Psi = 0, \quad (2)$$

$$\mathcal{E}(\mathbf{R}, Y = \pm h/2, u) = 0, \quad (3)$$

where  $u = ct$ ,  $c$  is the speed of light,  $\dot{\phantom{x}} = d/du$ ,  $\square = \Delta - \partial_u^2$ , and

$$S(\mathbf{R}, u) = Z_0 Q \begin{pmatrix} c\partial_Z \rho + \partial_u J_Z \\ c\partial_X \rho + \partial_u J_X \\ \partial_X J_Z - \partial_Z J_X \end{pmatrix}, \quad (4)$$

$$\dot{\mathbf{R}} = \mathbf{P}/m\gamma(P)c,$$

$$\dot{\mathbf{P}} = \frac{q}{c} [\mathbf{E}_{\parallel}(\mathbf{R}, Y, u) + (c\dot{\mathbf{R}} \times \mathbf{B}_Y(\mathbf{R}, Y, u))]. \quad (5)$$

Here  $Z_0$  is the free space impedance,  $Q$  is the total charge,  $QH(Y)\rho(\mathbf{R}, u)$  is the lab frame charge density (with  $\int H dY = \int \rho d\mathbf{R} = 1$ ),  $QH(Y)(J_Z, J_X)(\mathbf{R}, u)$  is the current density (which, of course, has no  $Y$  component),  $m$  is the electron mass,  $q$  is the electron charge (so that  $Q = Nq$  where  $N$  is the number of particles in the bunch),  $\gamma$  is the Lorentz factor,  $\mathbf{E}_{\parallel} = (E_Z, E_X)$  and  $\mathbf{B}_Y = (B_{ext}(\mathbf{R}) + B_Y(\mathbf{R}, Y, u))\mathbf{e}_Y$ . Equations (1-2) are incomplete without the coupling between  $S$  and  $\Psi$  given by

$$\rho(\mathbf{R}, u) := \int d\mathbf{P} \Psi(\mathbf{R}, \mathbf{P}, u), \quad (6)$$

$$\mathbf{J}_{\parallel}(\mathbf{R}, u) := \int d\mathbf{P} (\mathbf{P}/m\gamma(P)) \Psi(\mathbf{R}, \mathbf{P}, u), \quad (7)$$

\*Work supported by DOE grants DE-FG02-99ER41104 and DE-AC02-76SF00515

<sup>†</sup> ellisonatmath.unm.edu

where  $\mathbf{J}_{\parallel} = (J_Z, J_X)$ . We use  $(c, Z_0)$  as our basic parameters instead of  $(\epsilon_0, \mu_0)$ , where  $Z_0^2 = \mu_0/\epsilon_0$ ,  $c^2 = 1/\mu_0\epsilon_0$ .

Integrating the Vlasov equation over  $\mathbf{P}$  and using (6-7) yields the continuity equation  $\partial_u \rho + \frac{1}{c} \nabla_{\mathbf{R}} \cdot \mathbf{J}_{\parallel} = 0$ . We are investigating energy conservation, a type of Poynting theorem, for our model. In addition, we would like to characterize the ISR and CSR in analogy with  $N$  particles under uniform motion on a circle using a Klimontovich source. In that model the particle positions are IID random variables with probability density  $f(\theta)$ , and one obtains  $P_{rad} = \sum_n [N + (N^2 - N)] \int f(\theta) e^{in\theta} d\theta |^2 \Re e Z_n$ . Here the first term is identified with the ISR and the second with CSR.

While we believe (1-7) is a good approximation to the full 6D dynamics at high energies where space charge effects are small, we are investigating ways to check this. Consider the 6D case and define  $\rho_3 := Q\delta(Y)\rho(\mathbf{R}, u)$ ,  $\mathbf{J}_3 := Q\delta(Y)(J_Z, J_X, 0)$  and  $\Psi_3 := \delta(Y)\delta(P_Y)\Psi(\mathbf{R}, \mathbf{P}, u)$ . Then plugging these into the 6D Vlasov-Maxwell system we find that (1-7) must be satisfied with  $H(Y) = \delta(Y)$ . This will also give wave equations for  $\mathcal{E}_{\perp} = (E_Y, B_Z, B_X)$  and we can investigate its size.

## FIELD FORMULA

Solving (1) with Dirichlet's boundary condition (3) and zero initial conditions,  $\mathcal{E}(\mathbf{R}, Y, u = u_0) = \partial_u \mathcal{E}(\mathbf{R}, Y, u = u_0) = 0$ , gives

$$\mathcal{E}(\mathbf{R}, Y, u) = -\frac{1}{4\pi} \int_{-(u-u_0)}^{u-u_0} d\eta G(\eta, Y) \int_{u_0}^{u-|\eta|} dv \times \int_0^{2\pi} d\theta S(\mathbf{R} + \sqrt{(u-v)^2 - \eta^2} \mathbf{e}_{\theta}, v), \quad (8)$$

for  $u \geq u_0$ ,  $|Y| \leq g$ ,  $\mathbf{e}_{\theta} = (\cos \theta, \sin \theta)$ , and

$$G(\eta, Y) = \sum_{p \geq 1} H_p \cos \alpha_p \eta \psi_p(Y), \quad \alpha_p = p\pi/h,$$

$$\psi_p(Y) = \sin \alpha_p(Y + g), \quad H_p = \frac{1}{g} \int_{-g}^g H(Y) \psi_p(Y) dY. \quad (9)$$

We emphasize that the integrand in our formula has no singularities and a retarded time calculation is not necessary.

Equation (8) was derived by the eigen expansion  $\mathcal{E} = \sum_p \mathcal{E}_p \psi_p(Y)$ , where each  $\mathcal{E}_p(\mathbf{R}, u)$  satisfies a nonhomogeneous Klein-Gordon equation. If  $\hat{\mathcal{E}}_p(\mathbf{R}, W, u) := \exp(i\alpha_p W) \mathcal{E}_p(\mathbf{R}, u)$  then  $\hat{\mathcal{E}}_p$  satisfies the nonhomogeneous wave equation, in  $(Z, X, W)$ , with zero initial data and no boundary conditions. The resulting 3D wave equation is solved using the retarded Green function. Making the temporal argument in the source an integration variable gets rid of the singularity and gives (8). The formula can also be derived by the more physical method of images starting from Eq.(6) in [1], taking proper account of the initial conditions and again making the temporal argument of the source an integration variable.

In principal the initial value problem for (1-3) should be solved with the actual physical initial conditions. However these are not known, so researchers often take  $u_0 = -\infty$ , assume the source is given a priori for  $(-\infty, \tilde{u}]$ , and then start the self-consistent calculation at  $\tilde{u}$ . For the bunch compressor, we choose  $\tilde{u} = 0$  as the time the bunch enters the chicane. For numerical integration the contribution from the source is neglected for  $v$  less than a certain cutoff,  $u_c$ , to give a finite interval of integration. Another view leading to (8) is to solve the initial boundary problem in terms of the unknown initial condition. This adds a homogeneous solution of (1) to (8). Then  $u_0$  is then chosen enough negative so that the homogenous solution has "passed through" the bunch compressor before the bunch arrives and thus can be ignored in the solution.

To reduce the computation time we can average (8) with respect to  $H(Y)$ . This reduces the (3+1)D space-time grid to (2+1)D. A further reduction is obtained by assuming the  $Y$  extent of the beam is small compared to  $h$ . This amounts to approximating  $H(Y)$  by  $\delta(Y)$ , which reduces the 3D integration to a 2D one. The order of the two approximations can be reversed by first letting  $H(Y) = \delta(Y)$ , and then averaging over  $Y$  (which amounts to setting  $Y = 0$ ). For  $H(Y) = \delta(Y)$ , (8) becomes

$$\mathcal{E}(\mathbf{R}, Y, u) = -\frac{1}{4\pi} \sum_k (-1)^k \int_{u_0}^{u-|Y-kh|} dv 1_{[u_0, \infty)}(v) \int_0^{2\pi} d\theta S(\mathbf{R} + \sqrt{(u-v)^2 - (Y-kh)^2} \mathbf{e}_{\theta}, v), \quad (10)$$

where  $1_I(v)$  is the indicator function of the interval  $I$ . This is the exact solution for the  $H = \delta$  case discussed in the introduction. Putting  $Y = 0$  gives the formula we use and the interest is in (10) for  $\mathbf{R}$  in the bunch at time  $u$ , i.e.,  $\mathbf{R} \approx \mathbf{R}_r(\beta_r u)$ .

An important feature of (10) is that the second argument of the source does not depend on  $\theta$  and the  $\theta$  integration depends only on the bunch at time  $v$ . For  $Y = 0$ , the  $\theta$  integration is over an arc centered at the observation point  $\mathbf{R}$  at time  $u$  with radius  $\sqrt{(u-v)^2 - (kh)^2}$  and whose extent is its intersection with the bunch at time  $v$ . This is illustrated in the Fig. 2 for  $k = 0$ . When  $v$  is close to  $u$  the two bunches overlap and the  $\theta$ -support of the source is large. However, for most  $v$  the  $\theta$ -support is small and it is important to determine the approximate support as shown in the figure. Currently the  $\theta$  integration is done with the superconvergent trapezoidal rule. The remaining  $v$ -integrand varies with  $v$ ,  $\mathbf{R}$  and  $u$  in ways we have not yet quantified and so use an adaptive integrator.

## BEAM FRAME

In our approach the Maxwell equations are solved in the lab frame and the Vlasov equation is solved in the beam frame. Here we discuss the beam frame coordinates and the transformation of the densities between the two frames.

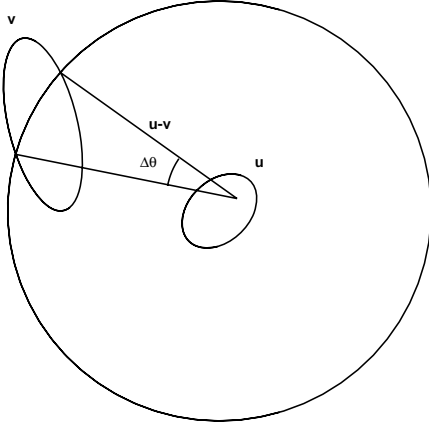
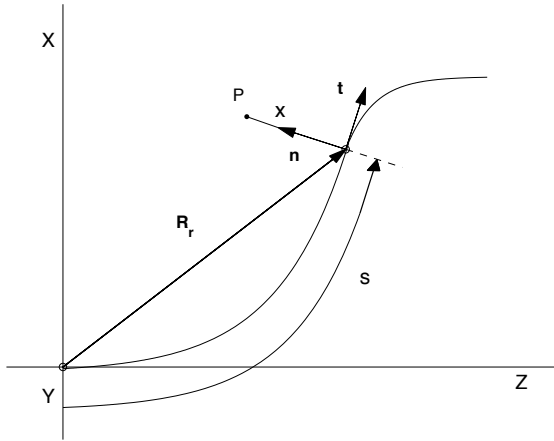

 Figure 2: Plan for  $\theta$  integration.


Figure 3: Beam frame coordinates.

The beam frame is defined in terms of the reference orbit using the Frenet-Serret coordinates  $(s, x)$ , where  $s$  is the arc length along the reference orbit and  $x$  is the perpendicular distance along  $\mathbf{n}$  from the orbit at  $\mathbf{R}_r(s)$  as shown in Fig. 3. Recall the reference orbit for a bunch compressor in Fig. 1.

The transformation  $(Z, X)$  to  $(s, x)$  is

$$\mathbf{R} = \mathbf{R}_r(s) + x\mathbf{n}(s), \quad (11)$$

where  $\mathbf{R}_r(s) := (Z_r(s), X_r(s))$  and the unit normal vector  $\mathbf{n}(s) := (-X'_r(s), Z'_r(s))$ . The corresponding tangent vector is  $\mathbf{t}(s) = \mathbf{R}'_r(s) = (Z'_r(s), X'_r(s))$ . In addition, we define  $p_s$  and  $p_x$  by  $\mathbf{P} := P_r(p_s\mathbf{t}(s) + p_x\mathbf{n}(s))$ , where  $P_r = m\gamma_r\beta_r c$  is the momentum of the reference particle. Finally, we define the curvature  $\kappa(s)$  by  $\mathbf{n}'(s) = \kappa(s)\mathbf{t}(s)$  and it follows that  $\mathbf{t}'(s) = -\kappa(s)\mathbf{n}(s)$ . In terms of Fig. 1 this makes  $\kappa$  negative in the first magnet, positive in the second and so on.

Our lab to beam transformation has three steps:

$$\begin{aligned} (Z, X, P_Z, P_X; u) &\rightarrow (s, x, p_s, p_x; u) \\ &\rightarrow (u, x, p_s, p_x; s) \rightarrow (z, x, p_z, p_x; s). \end{aligned} \quad (12)$$

The first step is the transformation just discussed, in the

second step the variables  $s$  and  $u$  are interchanged making  $s$  the new independent variable and in the final step  $z := s - \beta_r u$  replaces  $u$  as a dependent variable and  $p_z := (\gamma - \gamma_r)/\gamma_r$  replaces  $p_s$ . (11) defines  $s = s(\mathbf{R})$  and  $x = x(\mathbf{R})$  so that  $z = z(\mathbf{R}, u) = s(\mathbf{R}) - \beta_r u$  and we have the identity  $\mathbf{R} \equiv \mathbf{R}_r(z(\mathbf{R}, u) + \beta_r u) + x(\mathbf{R})\mathbf{n}(z(\mathbf{R}, u) + \beta_r u)$ . Now  $z$  is small in the bunch and expanding for small  $z$  gives  $\mathbf{R} = \mathbf{R}_r(\beta_r u) + M(\beta_r u)\mathbf{r} + O(\kappa(z^2 + xz))$  and we obtain the approximate inverse  $\mathbf{r} = M^T(\beta_r u)(\mathbf{R} - \mathbf{R}_r(\beta_r u))$ . Here  $M(s) = (\mathbf{t}(s), \mathbf{n}(s))$  and  $\mathbf{r} = (z, x)^T$ .

The equations of motion in  $(z, x, p_z, p_x; s)$  have the fields  $\mathcal{E}(\mathbf{R}, u)$  evaluated at  $\mathbf{R} = \mathbf{R}_r(s) + x\mathbf{n}(s)$  and  $u = (s - z)/\beta_r$ . We have the following approximations  $\mathcal{E}(\mathbf{R}_r(s) + x\mathbf{n}(s), (s - z)/\beta_r) \approx \mathcal{E}(\mathbf{R}_r(s + z) + x\mathbf{n}(s + z), s/\beta_r) \approx \mathcal{E}(\mathbf{R}_r(\beta_r u) + M(\beta_r u)\mathbf{r}, s)$ . At the first approximation we use the fact that the fields are slowly varying in  $s$  for fixed  $\mathbf{r}$ . The second approximation uses the fact that  $\beta_r \approx 1$  and we are only interested in the fields in the bunch for  $\mathbf{r}$  small. We obtain

$$\begin{aligned} z' &= -\kappa(s)x & p'_z &= F_{z1}(\hat{\mathbf{R}}, s) + p_x F_{z2}(\hat{\mathbf{R}}, s) \\ x' &= p_x & p'_x &= \kappa(s)p_z + F_x(\hat{\mathbf{R}}, s), \end{aligned} \quad (13)$$

where  $\hat{\mathbf{R}} := \mathbf{R}_r(s) + M(s)\mathbf{r}$  and  $' = d/ds$ . The self-forces are given approximately by

$$\begin{aligned} F_{z1} &= \frac{q}{P_{r,c}} \mathbf{E}_{\parallel} \cdot \mathbf{t}(s), & F_{z2} &= \frac{q}{P_{r,c}} \mathbf{E}_{\parallel} \cdot \mathbf{n}(s) \\ F_x &= \frac{q}{P_{r,c}} (-E_Z X'_r(s) + E_X Z'_r(s) - cB_Y), \end{aligned} \quad (14)$$

where  $(E_Z, E_X, B_Y)$  are evaluated at  $(\hat{\mathbf{R}}, s)$ . We have expanded  $F_x$  in order to point out that each of the last two terms are large whereas their difference is small.

The equations of motion (13), without the self fields, have been linearized. They can be solved and the solution written  $\zeta = \Phi(s)\zeta_0$ , where  $\zeta = (z, x, p_z, p_x)^T$ . Here  $\Phi$  is the principal solution matrix which is defined in terms of the dispersion function,  $D(s)$ , and  $R_{56}(s)$  (see [2]). The equations of motion in the interaction picture become

$$\zeta'_0 = \Phi^{-1}(s)(0, F_z, 0, F_x)^T(s, \zeta_0). \quad (15)$$

$\Phi(s)$  varies more slowly than the self-forces and so we numerically solve these rather than (13). A larger time step, which is controlled entirely by the self-forces, can be used.

Our field formula is in the lab frame so the lab charge and current densities must be determined from the beam frame PSD. The relation between lab and beam PSDs is

$$\Psi_L(Z, X, P_Z, P_X; u) = \frac{\beta_r^2}{P_r^2} f_B(z, x, p_z, p_x; s). \quad (16)$$

This leads to

$$\rho_L(\mathbf{R}; u) \approx \int dp_z dp_x f_B =: \rho_B(\mathbf{r}; s), \quad (17)$$

$$\mathbf{J}_L(\mathbf{R}; u) \approx \beta_r c [\rho_B(z, x; s)\mathbf{t}(s) + \tau(z, x; s)\mathbf{n}(s)], \quad (18)$$

where  $\tau(z, x; s) = \int p_x f_B(z, x, p_z, p_x; s) dp_z dp_x$ . Using the fact that  $f_B(z, x, p_z, p_x; \cdot)$  is slowly varying

and  $\rho_B(\mathbf{r}, s)$  has its support for  $\mathbf{r}$  small, we have  $\rho_B(z(\mathbf{R}, u), x(\mathbf{R}, u); z(\mathbf{R}, u) + \beta_r u) \approx \rho_B(\hat{\mathbf{r}}; \beta_r u)$ , where  $\hat{\mathbf{r}} = M^T(\beta_r u)(\mathbf{R} - \mathbf{R}_r(\beta_r u))$ . Thus

$$\rho_L(\mathbf{R}; u) \approx \rho_B(\hat{\mathbf{r}}; \beta_r u) \quad (19)$$

$$\begin{aligned} \mathbf{J}_L(\mathbf{R}; u) &\approx \beta_r c [\rho_B(\hat{\mathbf{r}}; \beta_r u) \mathbf{t}(z + \beta_r u) + \\ &\tau(\hat{\mathbf{r}}; \beta_r u) \mathbf{n}(z + \beta_r u)], \end{aligned} \quad (20)$$

where the  $\mathbf{J}_L$  approximation is derived similarly to that for  $\rho_L$ .

There is a subtlety in the second transformation caused by interchanging the roles of  $u$  and  $s$  as independent and dependent variables. The phase space density transformation and the approximations are discussed in detail in [3].

## UNPERTURBED SOURCE MODEL (UPS)

In this model we uncouple the Vlasov-Maxwell system so that it becomes a Liouville-Maxwell system. Here the source evolves with no self-fields and the fields are calculated from this unperturbed source. The Vlasov equation thus becomes a Liouville equation which defines the evolution of the beam frame phase space density.

We have focused on the bunch compressor with an initial Gaussian PSD density in the beam frame. Because (13) with out self-forces is a linear system, the unperturbed PSD is Gaussian at each  $s$  and thus the Lab frame charge density in (19) is Gaussian. This fact speeds up the field calculation considerably. We define an  $\{s_i\}$  grid along the reference orbit and a  $(Z, X)$  grid at each  $s_i$  which contains the bunch and is based on the evolution of the unperturbed charge density. We then calculate the self-forces (14) on this grid. We could integrate the Liouville equation using the method of local characteristics discussed below. To date we have proceeded as follows. We generate an initial ensemble of beam frame phase space points. We then move the points from  $s_i$  to  $s_{i+1}$  using (15) with the self-forces at  $s_i$ . We interpolate to determine the self-forces at points off the  $(Z, X)$  grid.

The UPS model is not self-consistent nor is it the first term in a systematic perturbation expansion in the size of the self-forces. Nevertheless, it has been helpful in the development of our self-consistent code because it is a good testing ground for our numerical and approximation procedures and computation with a Gaussian is fast. Furthermore, it may give a good approximation to the self-consistent case in some parameter range, [4, 5, 6].

Two particular points are worth mentioning. Our study of the UPS has given us insight into how to construct a space-time grid for the SCMC algorithm described below. In addition, we have found that for certain parameters, e.g., a small uncorrelated energy spread, a moving grid will be necessary for the PSD.

## SELF-CONSISTENT VLASOV-MAXWELL ALGORITHMS

We have discussed our method for calculating the fields in the lab frame and the determination of the lab frame charge and current densities from the beam frame PSD. Here we discuss two approaches for coupling the numerical integration of the Vlasov equation with field calculation.

### Self-Consistent Monte Carlo (SCMC) Method

Here the basic algorithm is the same as in the UPS case except the field calculation cannot be done up front and  $\rho_L$  can not be computed analytically. We discuss the basic algorithm and contrast it with the PIC method used in Vlasov-Poisson codes.

1. We generate an ensemble of IID phase space points from the density  $f_B(z, x, p_z, p_x; 0)$  using the rejection method. As an improvement we investigate a Quasi-Monte Carlo approach “which seeks to construct a set of initial points that perform significantly better than the average of a Monte Carlo approach”, see [7]. A similar procedure could be used in a PIC code.
2. We create a *globally smooth* lab frame charge density from the scattered beam frame phase space points. We fit the data with a finite Fourier series where the Fourier coefficients are calculated, as in Monte Carlo integration, from the scattered data. This is a technique used in statistical estimation, see e.g., [8]. We have found that a smooth representation is quite important as Borland found for Elegant before us. Note that this is a meshless procedure in contrast to the charge deposition of a PIC code.
3. We calculate the fields from the history of the Fourier coefficients using our field formula in (10). In a PIC code the Poisson equation is solved at this step (of course, the history of the beam is not needed).
4. We use 3) to advance the particles in the interaction picture of (15). In a PIC code 3) is also used to advance the particle positions.
5. The procedure is iterated going back to 2.

We note that our approach can treat a Vlasov-Poisson system as a special case. Also, our method is not a macroparticle method in the sense of modeling an  $N$  particle bunch with  $M \ll N$  macroparticles and letting them interact as point particles. We assume the electron bunch is well approximated by a continuum evolved by the Vlasov equation and hope that our algorithm approximates the true Vlasov dynamics. This is analogous to Monte Carlo integration where convergence follows from the strong law of large numbers and the central limit theorem and we hope to prove convergence. However, even though we expect convergence, the calculation of the PSD is probably beyond current or near future computing capability.

A parallel code has been developed and results for a bunch compressor are presented in [6].

### Method of local characteristics

The beam frame Vlasov equation is given by

$$\partial_s f + z' \partial_z f + x' \partial_x f + p'_z \partial_{p_z} f + p'_x \partial_{p_x} f = 0, \quad (21)$$

using (13-14). The basic idea of the method of local characteristics for an arc length step from  $s \rightarrow s + \Delta$  is quite simple: (i) let values of (14) on the interval  $[s, s + \Delta]$  be the value at  $s$ . Thus the Vlasov equation becomes a Liouville equation on that interval, (ii) The Liouville equation can then be solved on that interval by the standard method of characteristics, which integrates (13) backward from  $s + \Delta$  to  $s$ . It's hard to imagine a better approach, as long as the collective force is not rapidly varying, since this approach preserves the geometry of the solutions.

We implement this method as follows. Assume that at  $s_i$  we have a phase space grid containing the bunch, the PSD on the grid and the self-fields on the projected spatial grid. We then determine a phase space grid at  $s_{i+1}$ , integrate these points back to  $s_i$  and place them in the grid at  $s_i$ . Since these points will generically not be grid points, the PSD at  $s_{i+1}$  can then be determined in terms of the PSD at  $s_i$  using interpolation. The source can now be constructed and the self-fields determined. The scheme is now iterated. A parallel implementation will be necessary.

We traced the numerical implementation of this method back to [9] in the seventies. In the late nineties Warnock developed this approach in a study of the saw tooth instability in [10]. Most of the work to date has been done in the 2D case. Warnock's code has been further developed by Venturini and it has been extended by Bassi in a stochastic dynamics study.

Applications to storage rings are reviewed in [11]. Recent work by Venturini *et al.* has been focused on longitudinal phase space for single-pass systems, in particular the linac and bunch compressors for an Xray FEL [12]. Space charge forces and an elemental description of CSR were included. The Vlasov solution required special coordinate changes owing to the long and thin distribution in phase space resulting from energy chirp. The resulting scheme is able to handle the question of microbunching with low computational noise, and thus represents a substantial advance over particle simulations.

## DISCUSSION

In [6] we discuss our SCMC results and compare them with our previous UPS results, [4]. The main point here is that we now have a self-consistent code which runs on a UNM parallel cluster and at NERSC. Somewhat surprisingly the UPS turns out to give quantitative agreement with our SCMC and other codes applied to the Zeuthen benchmark at 5GeV. This is discussed in detail in [4, 5, 6]. We

expected big differences at 500 MeV because collective effects should be stronger, and while we find significant differences, the UPS calculation is still a worthwhile first approximation to the SCMC results. For these comparisons we had a Gaussian source with linear chirp, evolving under lattice dynamics. We have preliminary results for the same with nonlinear chirp and a parabolic density in  $z$ .

Our biggest strategic challenge at present is to develop the Vlasov technique for single-pass systems, with 4D phase space and energy chirp. Vlasov solutions in 4D have already been done by Sobol [13], for the coherent beam-beam interaction. There the meshing problems and complexity of the distribution are not severe, and programming the force calculation (by a Poisson solver) is much simpler. On the other hand, the time of integration is very much longer. We hope that in our single-pass problem the relatively short time of integration, combined with coordinate changes and the interaction picture, will lead to feasible calculations. Since a large time is required for the force calculation, we must devote more work to optimizing that part of the algorithm. For that the 1D source model [14] may provide insights as well as fast force evaluations for exploratory work.

## REFERENCES

- [1] R. Warnock, G. Bassi, J.A. Ellison, Nucl. Instr. and Meth. A 558(2006) 85-89.
- [2] S. Heifets, G. Stupakov, S. Krinsky, Phys. Rev. ST Accel. Beams 5 (2002) 064401
- [3] G. Bassi, J.A. Ellison, R. Warnock, "Relation of phase space densities in laboratory and beam centered coordinates", to be submitted.
- [4] G. Bassi, J.A. Ellison, K. Heinemann, EPAC06, Edinburgh, June 2006.
- [5] G. Bassi, J.A. Ellison, K. Heinemann, R. Warnock, "Coherent Synchrotron Radiation from Arbitrary Planar Orbits: A Vlasov-Maxwell Approach", in progress.
- [6] G. Bassi, J.A. Ellison, K. Heinemann, R. Warnock, PAC07, Albuquerque, June, 2007.
- [7] H. Niederreiter, "Random Number Generation and Quasi-Monte Carlo Methods", SIAM, 1992
- [8] S. Efromovich, "Nonparametric Curve Estimation: Methods, Theory, and Applications", Springer, 1999.
- [9] C.Z. Cheng, G. Knorr, J. Comp. Phys. 22(1976)330.
- [10] R. Warnock, J.A. Ellison, in: The Physics of High Brightness Beams, World Scientific, Singapore, 2000, also SLAC-PUB-8404(2000).
- [11] R. Warnock, Nucl. Instr. and Meth. A 561(2006) 186-194.
- [12] M. Venturini, R. Warnock, A. Zholents, Phys. Rev. ST Accel. Beams, 10, 054403(2007).
- [13] A. Sobol, Ph.D. Dissertation, University of New Mexico, July, 2006.
- [14] R. Warnock, PAC07, Albuquerque, June, 2007.